Temporal Frequency Tuning Reveals Interactions between the Dorsal and Ventral Visual Streams

Stephanie Kristensen[1], Frank E. Garcea[2], Bradford Z. Mahon[2], and Jorge Almeida[1]

Abstract

■ Visual processing of complex objects is supported by the ventral visual pathway in the service of object identification and by the dorsal visual pathway in the service of object-directed reaching and grasping. Here, we address how these two streams interact during tool processing, by exploiting the known asymmetry in projections of subcortical magnocellular and parvocellular inputs to the dorsal and ventral streams. The ventral visual pathway receives both parvocellular and magnocellular input, whereas the dorsal visual pathway receives largely magnocellular input. We used fMRI to measure tool preferences in parietal cortex when the images were presented at either high or low temporal frequencies, exploiting the fact that parvocellular channels project principally to the ventral but not dorsal visual pathway. We reason that regions of parietal cortex that exhibit tool preferences for stimuli presented at frequencies characteristic of the parvocellular pathway receive their inputs from the ventral stream. We found that the left inferior parietal lobule, in the vicinity of the supramarginal gyrus, exhibited tool preferences for images presented at low temporal frequencies, whereas superior and posterior parietal regions exhibited tool preferences for images present at high temporal frequencies. These data indicate that object identity, processed within the ventral stream, is communicated to the left inferior parietal lobule and may there combine with inputs from the dorsal visual pathway to allow for functionally appropriate object manipulation. ■

INTRODUCTION

Visual object processing can be separated into two distinct streams: a ventral stream, projecting from primary visual cortex (V1) to ventro-temporal regions, responsible for object identification, and a dorsal stream, projecting to posterior parietal cortex, responsible for the processing of object-directed actions and visuomotor control (e.g., Goodale & Milner, 1992). The dorsal stream can be further separated into a dorso-dorsal stream, including the superior parietal lobe, focused on online visuomotor control of actions, and a ventro-dorsal stream, including the inferior parietal lobe, critical for the representation of complex actions (Rizzolatti & Matelli, 2003; see also Binkofski & Buxbaum, 2013).

Object recognition and optimal visuomotor interactions with objects require information from both the ventral and dorsal streams to be brought into register. In particular, using an object correctly according to its function requires access to the visuomotor computations performed over the volumetric properties of that object, typical of the dorsal stream, as well as access to ventral stream information regarding the identity of the target object, and its canonical function. Exactly how those distinct types of information are integrated remains unclear. Here, we will focus on where in the left parietal lobule these channels of information interact during visual processing of manipulable objects (i.e., tools).

Vision is a highly segregated system, and two main subcortical pathways have been consistently demonstrated—the magnocellular (M) and parvocellular (P) pathways—that separate already in the retina. Retinal midget ganglion cells project to parvocellular layers of the lateral geniculate nucleus (LGN), whereas retinal parasol ganglion cells project to the magnocellular layers of the LGN (e.g., Livingstone & Hubel, 1988). Importantly, magnocellular and parvocellular pathways project differentially to the ventral and dorsal streams. The parvocellular pathway projects mainly to regions within the ventral stream, whereas the magnocellular pathway projects to both dorsal and ventral stream regions (Merigan & Maunsell, 1993; Ferrera, Nealey, & Maunsell, 1992).

This asymmetry in the projection of magnocellular and parvocellular inputs to the dorsal and ventral streams can be leveraged to test where the two streams come into register. Specifically, if we see signatures of parvocellular processing within regions of parietal cortex, then that would suggest that those parietal regions receive information from the ventral (and not the dorsal) visual pathway (for prior work within this framework, see Almeida, Fintzi, & Mahon, 2013; Mahon, Kumar, & Almeida, 2013). In this study, we capitalize on the fact that magnocellular and parvocellular pathways have dissociable temporal frequency preferences: Magnocellular cells have high temporal

[1]University of Coimbra, [2]University of Rochester

© 2016 Massachusetts Institute of Technology

Journal of Cognitive Neuroscience 28:9, pp. 1295–1302
doi:10.1162/jocn_a_00969

resolution allowing them to detect stimuli at high temporal frequencies (HTFs; such as flickering or fast motion), with highest sensitivity at temporal frequencies between 10 and 20 Hz (Derrington & Lennie, 1984). In comparison, parvocellular cells have a sustained response pattern and thus show a preference for slow-moving or static stimuli and respond more strongly to stimuli at lower temporal frequencies up to 10 Hz with a steep decrease in the ability to respond to frequencies at and above 10 Hz (Livingstone & Hubel, 1988; Derrington & Lennie, 1984). As such, temporal frequencies below 10 Hz (low temporal frequencies [LTFs]) are better processed by the parvocellular pathway, whereas temporal frequencies above 10 Hz (and especially between 10 and 20 Hz, HTFs) are differentially resolvable by the magnocellular pathway. Those temporal frequency preferences, initially established in the macaque, have also recently been shown to obtain in the human brain. Denison, Vu, Yacoub, Feinberg, and Silver (2014) demonstrated that using visual stimuli flickering at 5 and 15 Hz elicited responses in the P and M layers of the human LGN, respectively.

Experiment

In our experiment, we presented sequences of pictures of tools or animals at different presentation rates. Specifically, we presented pictures at LTFs or at HTFs to differentially excite the parvocellular and magnocellular pathways, respectively. We then tested how tool preferences within parietal areas are modulated by the temporal frequency at which the stimuli were presented. If we see areas within parietal cortex that respond more to tool items than control (i.e., animal) items when these items are presented at LTFs typical of parvocellular pathways, then we can conclude that those areas receive their inputs by way of a ventral visual pathway analysis of the input and not a dorsal visual pathway analysis.

METHODS

Participants

Twenty participants were tested, of which 19 completed eight experimental runs and one completed six runs (14 women). All participants were right-handed, had normal or corrected-to-normal vision, and had no history of neurological disorders. The project was approved by the ethical committee of the Faculty of Medicine, University of Coimbra.

Experimental Stimuli

Stimuli were grayscale pictures of animals and tools. Twelve animal and 12 tool items were used, with 20 exemplars for each item (total of 480 pictures). The stimuli were 400 × 400 pixels in size (~10° of visual angle) and were presented on a gray background, using an Avotec (Stuart, FL) projector at a 60-Hz refresh rate. Colored images were collected from the World Wide Web and internal image databases and converted to grayscale. Items used were as follows: animals = bear, cat, cow, dog, horse, owl, panda, pigeon, rabbit, raccoon, sheep, and tiger; tools = bat, broom, corkscrew, flashlight, flyswatter, hammer, paintbrush, pen, scissors, screwdriver, shovel, and stapler.

General Procedure

A "simple framework" (Schwarzbach, 2011) was used to control stimulus presentation in Psychtoolbox in MATLAB (The MathWorks, Natick, MA) running on Windows 7 (Brainard, 1997). Stimuli were back-projected on a screen that participants viewed with a mirror attached to the head coil. Participants viewed the tool and animal stimuli passively (no response) in a miniblock design. Our design consisted of 2 categories (animals and tools) × 4 presentation rates (5, 10, 15, and 30 Hz) for a total of eight conditions. Each miniblock represented one cell of the design and lasted 8 sec. Miniblocks of stimuli were separated by 8 sec of fixation. The 240 items for each category were repeated twice within the design: Each image from a given category was presented once in the 30-Hz condition (all 240 items) and once again across the remaining three conditions (40 items in the 5-Hz condition, 80 items in the 10-Hz condition, and 120 items in the 15-Hz condition). Miniblocks were then pseudorandomized within each run so that no more than two miniblocks of the same category occurred consecutively. Each run contained two repetitions of the design, or 16 miniblocks in total, and lasted approximately 4 min 40 sec. The speeds of 5, 10, 15, and 30 Hz corresponded to image presentation durations of 200, 100, 67, and 33 msec per image, respectively. Between either Runs 3 and 4, or Runs 4 and 5, participants completed an experimental run to map population receptive fields (data not reported herein).

MRI Parameters

Whole-brain BOLD imaging was conducted on a Siemens (Berlin, Germany) Tim Trio 3-T MRI scanner with a 12-channel head coil at the Portuguese Brain Imaging Network. High-resolution structural T1 contrast images were acquired using a magnetization prepared rapid gradient-echo pulse sequence at the start of each session (repetition time = 2530 msec, echo time = 3.29 msec, flip angle = 7°, field of view = 256 mm, matrix = 256 × 256, 1 × 1 × 1 mm ascending interleaved slices). An EPI pulse sequence was used for T2* contrast (repetition time = 2000 msec, echo time = 30 msec, flip angle = 90°, field of view = 256 mm, matrix 256 × 256, 30 ascending interleaved even–odd slices, voxel size = 1 × 1 × 1 mm). The first two volumes of each run were discarded to allow for signal equilibration.

fMRI Data Analysis

fMRI data were analyzed with the Brain Voyager software package 2.8.1 and in-house scripts drawing on the BVQX toolbox for MATLAB. Preprocessing of the functional data included, in the following order, slice scan time correction (sinc interpolation), motion correction with respect to the first volume of the first functional run, and linear trend removal in the temporal domain (cutoff: two cycles within the run). Functional data were registered (after contrast inversion of the first volume) to high-resolution deskulled anatomy on a participant-by-participant basis in native space. For each participant, echo-planar and anatomical volumes were transformed into standardized (Talairach & Tournoux, 1988) space. Functional data were smoothed at 6-mm (1.5 voxels) FWHM and interpolated to 3 × 3 × 3 mm voxels. The general linear model was used to fit beta estimates to the events of interest. The first derivatives of 3-D motion correction from each run were added to all models as regressors of no interest to attract variance attributable to head movement. All analyses treated participants as a random factor, and there were thus 19 degrees of freedom in the group-level analyses. Experimental events were convolved with a standard two-gamma hemodynamic response function. There were eight (2 × 4) regressors: the category of the stimulus (tools and animals) and the presentation rate of images (5, 10, 15, and 30 Hz).

We computed an ANOVA with two within-participant factors: Category (tool vs. animal) and Presentation rate (5, 10, 15, and 30 Hz). From this, we inspected left parietal cortex for regions exhibiting an interaction between these two factors. We then focused on testing the simple effects and computed four contrasts to look for stronger neural activation for tools than animals at each presentation rate. On the basis of the prior literature in humans (Denison et al., 2014), we then focused on two of those simple contrasts: We focused on tool preferences by comparing neural activation for tools and animals when both stimulus types were presented at temporal frequencies within the parvocellular response spectrum ($Tools_{[5\ Hz]} > Animals_{[5\ Hz]}$) or within the magnocellular response spectrum ($Tools_{[15\ Hz]} > Animals_{[15\ Hz]}$).

RESULTS

Inferior-to-Superior Organization of Tool Preferences by Temporal Frequency within Parietal Cortex

We first conducted a two-way ANOVA with Category (tool vs. animals) and Presentation rate (5, 10, 15, and 30 Hz) as within-participant factors to test whether responses within left parietal cortex to tool items, compared with animal items, were dependent on the presentation rate at which the target pictures were presented. Figure 1A shows the activation map obtained for the interaction between those two factors (cluster corrected at $p \leq .05$). As can be seen in this figure, an extensive left parietal

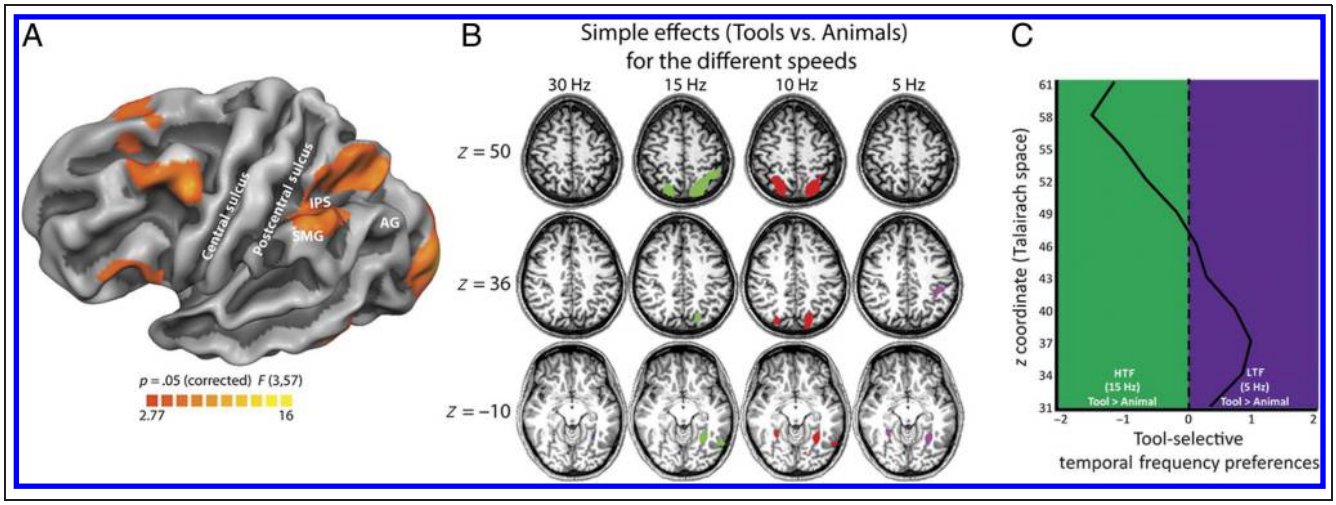

Figure 1. Inferior-to-superior organization of left parietal cortex by temporal frequency-dependent tool preferences. (A) Map of the interaction between the two within-participant factors of Category and Presentation rate. An extensive left parietal region was identified. (B) Volume maps of the four simple effects contrasting tools and animals at the different presentation rates. Talairach z values correspond to locations that are typical of some of the landmarks of the tool network. Blue patches correspond to voxels that show stronger activity for tool than animals under 30 Hz, green patches correspond to voxels that show stronger activity for tool than animals under 15 Hz, red patches correspond to voxels that show stronger activity for tool than animals under 10 Hz, and purple patches correspond to voxels that show stronger activity for tool than animals under 5 Hz. All maps thresholded at FDR $q < 0.05$. (C) The parietal region was further studied to understand whether HTF- and LTF-dependent tool preferences were differentially distributed along the inferior-to-superior dimension. Thus, the left parietal interaction region was sliced in 3-mm planes along the z dimension covering the area between $z = 31$ and $z = 61$ (y axis in the plot). For each slice, the average t values for tool preferences for the two key temporal frequencies (5 and 15 Hz) were calculated and subtracted such that positive values on the x axis indicate higher t values for the LTF tool-specific contrast than for the HTF one, whereas negative values on the x axis indicate higher t values for the HTF tool-specific contrast than for the LTF one. AG = angular gyrus; IPS = intraparietal sulcus; SMG = supramarginal gyrus.

area was obtained, spanning parts of the inferior parietal lobule (i.e., the supramarginal gyrus) and superior parietal lobule as well as parts of the intraparietal sulcus.

We then tested tool preferences within each presentation rate and computed four simple effects contrasting tools with animals for each speed (5, 10, 15, and 30 Hz). As can be seen in Figure 1B (all maps thresholded at false discovery rate [FDR] $q < 0.05$), tools elicited stronger activity in medial aspects of the left fusiform gyrus under all presentation rates. However, there were differences in how parietal cortex responded to tools (when compared with animals) at the different speeds. In particular, certain speeds elicited tool-specific activity within more superior aspects of parietal cortex (i.e., the simple contrast for 10 and 15 Hz) or in more inferior aspects (i.e., the simple contrast for 5 Hz) or failed to elicit any differential activity (i.e., the simple contrast for 30 Hz).

Importantly, because we were interested in how different regions within tool-sensitive parietal cortex processed M- and P-biased input, we focused on characterizing tool preferences under M- and P-related speeds. For this, we further inspected the simple effects that have been established as optimal for eliciting P- and M-biased processing and tested these simple effects (Tools > Animals) within the parietal region obtained from our ANOVA. For the P-biased tool contrast, because the parvocellular pathway prefers LTFs below 10 Hz, we inspected tool preferences (i.e., voxels presenting higher activation for tools when compared with animals) when all stimuli (tools and animals) were presented at 5 Hz (see also Denison et al., 2014). To identify tool preferences that are communicated via the magnocellular-dominated dorsal stream, and because the magnocellular pathway prefers HTFs, in particular between 10 and 20 Hz, we explored tool preferences when all stimuli were presented at 15 Hz (see also Denison et al., 2014). Importantly, these contrasts, which show tool preferences separately for HTF and LTF, are entirely independent from one another—thus, there is nothing about this analysis approach that would bias against observing completely overlapping voxels as exhibiting tool preferences for 5- and 15-Hz presentation rates.

The left parietal region presented in Figure 1A was sliced into 3-mm thick planes along the inferior-to-superior plane (i.e., along the z dimension) to capture the divide between superior and inferior aspects of parietal cortex. We treated each slice as a separate ROI and extracted the t values for each of our two simple contrasts ($\text{Tools}_{[5\ \text{Hz}]} > \text{Animals}_{[5\ \text{Hz}]}$ and $\text{Tools}_{[15\ \text{Hz}]} > \text{Animals}_{[15\ \text{Hz}]}$). These t values were compared to ascertain whether, at each slice along the inferior-to-superior dimension, tool preferences presented different biases (i.e., M and P). As can be seen in Figure 1C, there is a clear divide in the M and P biases for the slices below and above $z = 46/49$, which corresponds well with the approximate location of the anterior intraparietal sulcus (for a review, see Garcea & Mahon, 2014). Below $z = 46/49$, t values for the simple effect of tools over animals under LTFs (5 Hz) are, on average, greater than those for tool preferences under HTFs (15 Hz); above $z = 46/49$, t values for LTF-dependent tool preferences tended to be, on average, less than those for HTF-dependent tool preferences.

We then further inspected these M and P simple effects at the whole-brain level. The resulting contrast maps, corrected for multiple comparisons using an FDR of 5% (i.e., all maps thresholded at FDR $q < 0.05$), are shown in Figure 2A. There were largely nonoverlapping regions of left parietal cortex responding differently to these two contrasts. Tool preferences for LTF presentations were observed in more inferior aspects of left parietal cortex principally within BA 40 (i.e., the supramarginal gyrus), whereas tool preferences for HTF presentations were observed in superior (i.e., BA 7) and posterior aspects of left parietal cortex. These findings are in extremely good agreement with prior work indicating an inferior-to-superior dissociation in left parietal tool-preferring regions by subcortical distinctions (Almeida et al., 2013; Mahon et al., 2013). In that prior work, we observed a very similar inferior-to-superior organization whereby inferior parietal regions exhibited tool preferences for stimuli defined by high spatial frequencies (Mahon et al., 2013) or isoluminant chromatic (red/green) information (Almeida et al., 2013). The current findings, using temporal frequencies, converge with those prior findings to indicate that tool preferences in the left inferior parietal lobule are contingent on analysis of the visual input by the ventral visual pathway.

Finally, we sought to compare how the regions we showed to be dependent on LTF or HTF fared with known anatomical and functional parcellations of parietal cortex (e.g., Caspers et al., 2006, 2008; Scheperjans, Eickhoff, et al., 2008; Scheperjans, Hermann, et al., 2008; Choi et al., 2006). First, we wanted to understand whether and how our interaction region and our contrasts of interest overlapped. Figure 2B shows a considerable amount of overlap between the two contrasts and the ROI obtained for the interaction between the category of the stimuli and the presentation rate at which the stimuli were presented. More importantly, Figure 2C shows the overlap of our contrasts of interest with the parcellations proposed by Caspers and colleagues (2006, 2008) for the inferior parietal lobule. According to Caspers and colleagues, the supramarginal gyrus encompasses five subregions that span this region across the posterior-to-anterior dimension: PFm, PF, PFcm, PFt, and PFop. Interestingly, our LTF P-biased tool-preferring region overlaps maximally with area PFt and, to a much lesser extent, with area PF; in contrast, our HTF M-biased tool-preferring regions show no overlap with any of the clusters within the supramarginal gyrus. Interestingly, PFt has been shown to be anatomically connected, among other areas, to anterior and posterior fusiform gyrus, regions within the intraparietal sulcus, and superior parietal areas (Caspers et al., 2011). Moving superiorly, Scheperjans and colleagues (Scheperjans, Eickhoff, et al., 2008; Scheperjans, Hermann,

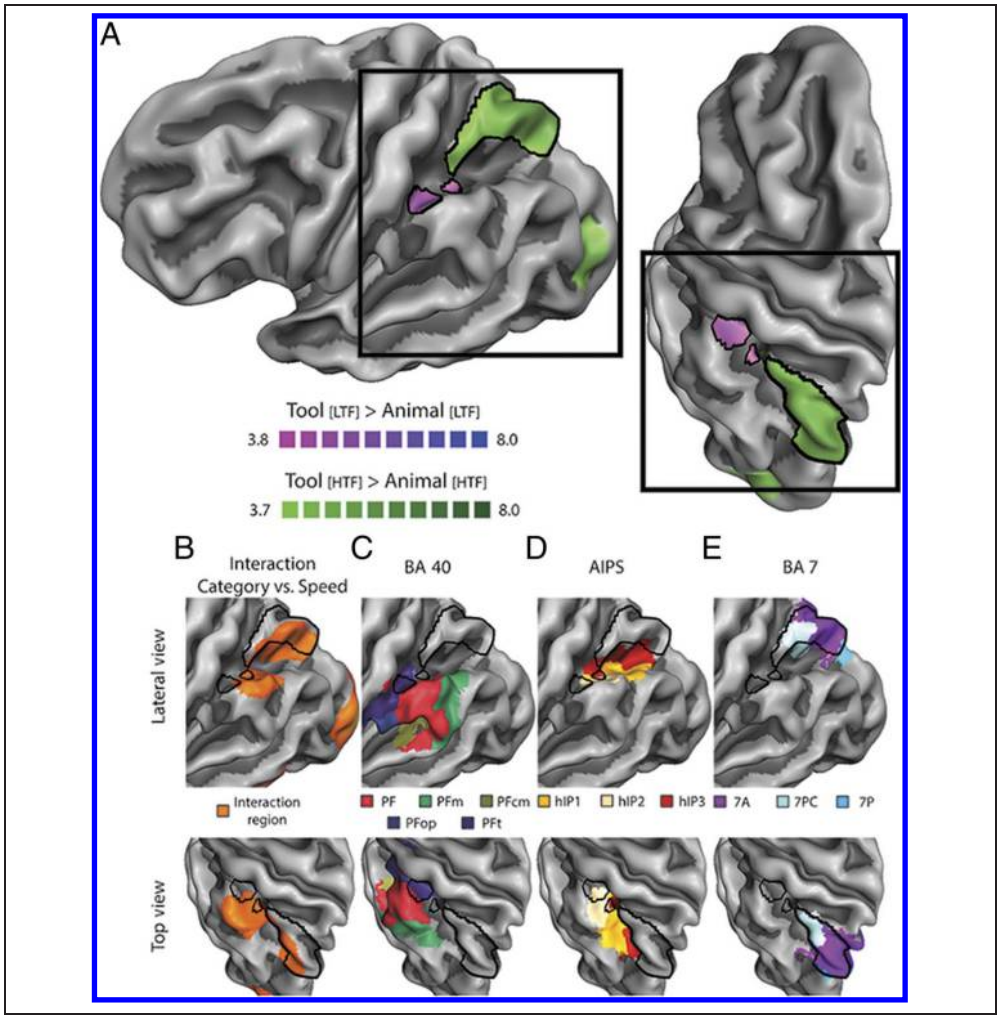

Figure 2. Temporal frequency-dependent tool preferences in parietal cortex. Tool-preferring regions within parietal cortex for different temporal frequency profiles. (A) We present two contrasts: $Tools_{[5\ Hz]} > Animals_{[5\ Hz]}$ (colored purple) and $Tools_{[15\ Hz]} > Animals_{[15\ Hz]}$ (colored green; both maps: $q < 0.05$, FDR corrected). We then overlaid our LTF and HTF tool-preferring regions on (B) the interaction region presented in Figure 1A; (C) the parcellations proposed by Caspers and colleagues (2006) of the left inferior parietal lobule (BA 40); (D) the parcellations of the intraparietal sulcus proposed by Choi et al. (2006) and Scheperjans et al. (Scheperjans, Eickhoff, et al., 2008; Scheperjans, Hermann, et al., 2008); and (E) the parcellations proposed by Scheperjans et al. (Scheperjans, Eickhoff, et al., 2008; Scheperjans, Hermann, et al., 2008) for the superior parietal lobule (BA 7). Those parcellations were based on the SPM Anatomy Toolbox (Eickhoff et al., 2005).

et al., 2008) and Choi and colleagues (2006) subdivided the human intraparietal sulcus into three regions: hIP1, hIP2, and hIP3. As can be seen in Figure 2D, there is not a lot of overlap between those parcellations and our contrasts. If anything, our P-biased tool preferences overlap minimally with the inferior lateral bank of the intraparietal sulcus around region hIP2, whereas our M-biased tool preferences overlapped with the superior aspect in the vicinity of hIP3. Finally, we also tested the overlap of our contrasts with clusters within the superior parietal lobule and specifically within BA 7. According to Scheperjans and colleagues (Scheperjans, Eickhoff, et al., 2008; Scheperjans, Hermann, et al., 2008), this Brodmann's area can be further parcellated into four clusters: 7A, 7P, 7PC, and 7M. Figure 2E shows that our M-biased tool contrast overlaps with areas 7A, P, and PC, whereas our P-biased tool contrast shows no overlap with any of these clusters.

It is important to note that these M and P simple effects show that pathway-biased tool preferences extend somewhat beyond the parietal region that was defined by the interaction between Presentation rate and Category (see Figures 1A and 2B). Nevertheless, it seems clear that the major results presented here still hold, albeit in a more spatially circumscribed fashion, even if we look only at the sites where the M and P simple contrasts and the interaction region overlap. That is, P-biased tool preferences are present in the PFt region within the supramarginal gyrus, and in parts of the hIPS (i.e., hIP2), whereas M-biased tool preferences are limited to areas within BA 7 (i.e., 7A and 7PC).

DISCUSSION

Here, we reported evidence that tool preferences in the inferior parietal lobule are contingent on inputs from the ventral visual pathway. We used images of tools and animals and presented them at different temporal frequencies to bias processing either toward the magnocellular or parvocellular pathways. The parvocellular pathway has greater sensitivity for LTFs and projects to the ventral visual pathway, whereas the magnocellular pathway has greater sensitivity for HTFs and projects to both the dorsal and ventral streams. Thus, in the measure to which tool-preferring regions of parietal cortex show stronger tool preferences for LTFs, it can be concluded that those regions receive their inputs from the ventral visual pathway.

We found that tool preferences under LTFs were restricted to the inferior parietal lobule, namely, within area PFt (a region within the supramarginal gyrus), whereas tool preferences under HTFs were present within the superior parts of the parietal lobe, namely, regions 7A, P, and PC within BA 7, and more posterior aspects of the parietal cortex. Because the parvocellular pathway projects to ventral and not dorsal stream structures, the observation that tool preferences in the inferior parietal lobule are carried by LTFs indicates that the inferior parietal lobule receives inputs during visual processing of tools from the ventral visual pathway. This does not preclude our LTF tool-preferring area from receiving M-biased information. As a matter of fact, the subdivision where our area lies—the ventro-dorsal stream—receives input from area MT/V5, a region that receives magnocellular input (Lyon, Nassi, & Callaway, 2010). It seems however that, when filtered through the constraint of exhibiting differential BOLD responses to tools compared with animals, there is a clear bias whereby the major input originates from P-biased ventral stream structures.

It is important to note that the seminal studies demonstrating different temporal frequency profiles for M and P pathways were conducted using very simple stimuli (i.e., gratings) and in nonhuman animals (e.g., owl monkey; Xu et al., 2001), whereas here we used complex objects and measured neural activity in humans. Importantly, Denison and colleagues (2014) demonstrated that the P and M layers of the human LGN are also excited by LTF and HTF, respectively—notably, the frequencies used by Denison and colleagues were the same as our frequencies of interest. Moreover, there are many differences between our HTF and LTF conditions (e.g., number of pictures presented in each condition) and between our categories of interest (e.g., tools are elongated, whereas most animals are not). Some of these differences were also true, however, for the experiments performed over simple stimuli (e.g., the number of alternations between the phases of the gratings used to separate M and P responses was necessarily different for HTF and LTF, as they were for our LTF and HTF sequences of pictures). Interestingly, other aspects that differ between our conditions should be explicitly addressed in future work, namely, the issue of elongation and how object elongation may be a basic feature that biases processing of a complex object within the ventral and dorsal streams (Almeida et al., 2014; Sakuraba, Sakai, Yamanaka, Yokosawa, & Hirayama, 2012; Almeida, 2010).

Our findings are in line with prior fMRI work by our group (Almeida et al., 2013; Mahon et al., 2013). Those studies explored how other neurophysiological characteristics of the same subcortical pathways affected tool preferences in parietal cortex. Specifically, those studies found that stimuli that contained only high spatial frequencies (Mahon et al., 2013), or were defined by isoluminant red/green differences (Almeida et al., 2013), led to tool preferences restricted to the left inferior parietal lobule. In contrast, tool preferences in superior and posterior parietal cortex were driven by low spatial frequencies (Mahon et al., 2013) and color distinctions (blue/yellow) carried by nonparvocellular pathways (e.g., the koniocellular pathway; Almeida et al., 2013). The results we have reported herein, together with those prior studies, shed new light on the interaction between the dorsal and ventral visual streams, as they illustrate that the computations occurring within the left inferior parietal lobule, presumably related to object manipulation knowledge (Chen, Garcea, & Mahon, 2015; Ishibashi, Lambon Ralph, Saito, & Pobric, 2011; Mahon et al., 2007; Boronat et al., 2005; Kellenbach, Brett, & Patterson, 2003), are contingent on analysis of the visual input by the ventral visual pathway (see also Garcea & Mahon, 2014; Binkofski & Buxbaum, 2013).

The data herein may be a manifestation of an important distinction proposed by Johnson and Grafton (2003) on the difference between "acting on" an object and "acting with" an object. Acting on an object refers to interacting with an object by treating the object as a manipulable entity, devoid of particular functions and manipulations, but focusing on the visuomotor aspects of the object such as its volumetric properties and its spatial relation with the effector. Acting with an object refers to exploiting the object's typical function and associated manner of manipulation, in the service of a goal. Interestingly, regions within the superior parietal lobule (and in the vicinity of our M-biased tool region) are of central importance for the kinds of processing that subserve acting on an object. For instance, this M-biased tool region shows some overlap with areas within parietal cortex that are responsible for extracting and computing 3-D shape (e.g., DIPSM, DIPSA, and POIPS; Durand, Peeters, Norman, Todd, & Orban, 2009; Georgieva, Peeters, Kolster, Todd, & Orban, 2009; Georgieva, Todd, Peeters, & Orban, 2008; Orban et al., 2003), perhaps suggesting a role in processing volumetric properties such as 3-D shape in the service of preparing a grasp and planning to manipulate an object. Regions within the inferior parietal lobule (and in the vicinity of our P-biased tool region) support the processes that are at play when acting with objects (Brandi, Wohlschläger, Sorg, & Hermsdörfer, 2014; Binkofski & Buxbaum, 2013; Rizzolatti & Matelli, 2003). Clearly, these data also seem to map onto the proposed subdivision of the dorsal pathway into dorso-dorsal and ventro-dorsal streams (Binkofski & Buxbaum, 2013; Rizzolatti & Matelli, 2003).

So how does our tool-selective region, which is contingent on the processing happening within the ventral stream, fit with the proposal of Johnson and Grafton (2003)? There seems to be overlap between our P-biased tool-preferring regions and those reported by Brandi et al. (2014) and Peeters, Rizzolatti, and Orban (2013). Those foci of activity are within the anterior parts of the supramarginal gyrus, more specifically in or around area PFt. Importantly, PFt seems to be coding aspects that are specific to tool-related actions, and not overall

hand actions, and be related with overlearned, function-specific manipulations of familiar tools (e.g., Brandi et al., 2014; Peeters et al., 2013). Our data further chart the complex processing within this region by demonstrating that this information is dependent on the processing happening within the ventral stream. This may be so, potentially, because of the need to retrieve the actual function of the object to map the associated manipulation and therefore implement the causal relationship between function, manipulation, and consequential use of a tool. This is also in line with the findings of Valyear and Culham (2010) that showed that neural responses to hand grasps that are contingent on the typical use of an object are obtained within ventral stream regions. Our data may also point to the fact that processing within the ventral stream facilitates the understanding of the technical properties that a target tool possesses (e.g., a sharp-toothed resistant surface) and that can be used to fulfill certain goals (e.g., to cut; Osiurak, Jarry, & Le Gall, 2010).

More generally, these considerations are in line with the suggestion that abstract information may be integrated with motor plans within the inferior parietal lobule (e.g., Arbib, 2008). The left inferior parietal lobule has long been associated with the planning of gestures and actions for tool use (e.g., Vingerhoets, Acke, Vandemaele, & Achten, 2009; Johnson-Frey, Newman-Norlund, & Grafton, 2005). Buxbaum, Kyle, Grossman, and Coslett (2007) and Arbib (2008) suggested that the inferior parietal lobule functions as an area of integration between object identity information from the ventral stream and spatial body representations processed within the dorsal stream. Possibly, this integration plays a major role in the selection and preparation of the appropriate motor manipulation when reaching toward objects. For example, consider reaching for a pen. Appropriate grasping of a pen will be dependent not only on the shape of the pen but also on the action to be executed. Picking up the pen for writing will elicit a different grasp compared with picking up the pen to pass it to someone. The left inferior parietal lobule has the connectivity and response characteristics to compute grasp information that is informed by the (often implicit) planned or anticipated use of the object.

Acknowledgments

This work was supported by a Foundation for Science and Technology of Portugal Project grant PTDC/MHC-PCN/3575/2012, and *programa COMPETE* to J. A. S. K. was supported by a research initiation grant from the Foundation for Science and Technology of Portugal Project (grant PTDC/MHC-PCN/3575/2012). Preparation of this manuscript was supported in part by NIH Grant R01 NS089609 to B. Z. M. F. E. G. was supported by a University of Rochester Center for Visual Science predoctoral training fellowship (NIH Training grant 5T32EY007125-24).

Reprint requests should be sent to Jorge Almeida, Faculty of Psychology and Educational Sciences, University of Coimbra, 3001-802 Coimbra, Portugal, or via e-mail: jorgealmeida@fpce.uc.pt.

REFERENCES

Almeida, J. (2010). *Unconscious processes reveal different circuits for visual object recognition*. Cambridge, MA: Harvard University Press.

Almeida, J., Fintzi, A. R., & Mahon, B. Z. (2013). Tool manipulation knowledge is retrieved by way of the ventral visual object processing pathway. *Cortex, 49,* 2334–2344.

Almeida, J., Mahon, B., Zapater-Raberov, V., Dziuba, A., Cabaço, T., Marques, J. F., et al. (2014). Grasping with the eyes: The role of elongation in visual recognition of manipulable objects. *Cognitive, Affective & Behavioral Neuroscience, 14,* 319–335.

Arbib, M. A. (2008). From grasp to language: Embodied concepts and the challenge of abstraction. *Journal of Physiology, Paris, 102,* 4–20.

Binkofski, F., & Buxbaum, L. J. (2013). Two action systems in the human brain. *Brain and Language, 127,* 222–229.

Boronat, C. B., Buxbaum, L. J., Coslett, H. B., Tang, K., Saffran, E. M., Kimberg, D. Y., et al. (2005). Distinctions between manipulation and function knowledge of objects: Evidence from functional magnetic resonance imaging. *Brain Research, Cognitive Brain Research, 23,* 361–373.

Brainard, D. H. (1997). The Psychophysics toolbox. *Spatial Vision, 10,* 433–436.

Brandi, M.-L., Wohlschläger, A., Sorg, C., & Hermsdörfer, J. (2014). The neural correlates of planning and executing actual tool use. *Journal of Neuroscience, 34,* 13183–13194.

Buxbaum, L. J., Kyle, K., Grossman, M., & Coslett, B. (2007). Left inferior parietal representations for skilled hand-object interactions: Evidence from stroke and corticobasal degeneration. *Cortex, 43,* 411–423.

Caspers, S., Eickhoff, S. B., Geyer, S., Scheperjans, F., Mohlberg, H., Zilles, K., et al. (2008). The human inferior parietal lobule in stereotaxic space. *Brain Structure & Function, 212,* 481–495.

Caspers, S., Eickhoff, S. B., Rick, T., von Kapri, A., Kuhlen, T., Huang, R., et al. (2011). Probabilistic fibre tract analysis of cytoarchitectonically defined human inferior parietal lobule areas reveals similarities to macaques. *Neuroimage, 58,* 362–380.

Caspers, S., Geyer, S., Schleicher, A., Mohlberg, H., Amunts, K., & Zilles, K. (2006). The human inferior parietal cortex: Cytoarchitectonic parcellation and interindividual variability. *Neuroimage, 33,* 430–448.

Chen, Q., Garcea, F. E., & Mahon, B. Z. (2015). The representation of object-directed action and function knowledge in the human brain. *Cerebral Cortex, 26,* 1609–1618.

Choi, H.-J., Zilles, K., Mohlberg, H., Schleicher, A., Fink, G. R., Armstrong, E., et al. (2006). Cytoarchitectonic identification and probabilistic mapping of two distinct areas within the anterior ventral bank of the human intraparietal sulcus. *Journal of Comparative Neurology, 495,* 53–69.

Denison, R. N., Vu, A. T., Yacoub, E., Feinberg, D. A., & Silver, M. A. (2014). Functional mapping of the magnocellular and parvocellular subdivisions of human LGN. *Neuroimage, 102,* 358–369.

Derrington, M., & Lennie, P. (1984). Spatial and temporal contrast sensitivities of neurones in lateral geniculate nucleus of macaque. *Journal of Physiology, 357,* 219–240.

Durand, J.-B., Peeters, R., Norman, F., Todd, J. T., & Orban, G. A. (2009). Parietal regions processing visual 3D shape extracted from disparity. *Neuroimage, 46,* 1114–1126.

Eickhoff, S. B., Stephan, K. E., Mohlberg, H., Grefkes, C., Fink, G. R., Amunts, K., et al. (2005). A new SPM toolbox for combining probabilistic cytoarchitectonic maps and functional imaging data. *Neuroimage, 25,* 1325–1335.

Ferrera, V. P., Nealey, T. A., & Maunsell, J. H. R. (1992). Mixed parvocellular and magnocellular geniculate signals in visual area V4. *Nature, 358,* 756–758.
Garcea, F. E., & Mahon, B. Z. (2014). Parcellation of left parietal tool representations by functional connectivity. *Neuropsychologia, 60,* 131–143.
Georgieva, S., Peeters, R., Kolster, H., Todd, J. T., & Orban, G. A. (2009). The processing of three dimensional shape from disparity in the human brain. *Journal of Neuroscience, 29,* 727–742.
Georgieva, S. S., Todd, J. T., Peeters, R., & Orban, G. A. (2008). The extraction of 3D shape from texture and shading in the human brain. *Cerebral Cortex, 18,* 2416–2438.
Goodale, M. A., & Milner, A. D. (1992). Separate visual pathways for perception and action. *Trends in Neurosciences, 15,* 20–25.
Ishibashi, R., Lambon Ralph, M. A., Saito, S., & Pobric, G. (2011). Different roles of lateral anterior temporal lobe and inferior parietal lobule in coding function and manipulation tool knowledge: Evidence from an rTMS study. *Neuropsychologia, 49,* 1128–1135.
Johnson, S. H., & Grafton, S. T. (2003). From "acting on" to "acting with": The functional anatomy of object-oriented action schemata. *Progress in Brain Research, 142,* 127–139.
Johnson-Frey, S. H., Newman-Norlund, R., & Grafton, S. T. (2005). A distributed left hemisphere network active during panning of everyday tool use skills. *Cerebral Cortex, 15,* 681–695.
Kellenbach, M. L., Brett, M., & Patterson, K. (2003). Actions speak louder than functions: The importance of manipulability and action in tool representation. *Journal of Cognitive Neuroscience, 15,* 30–46.
Livingstone, M., & Hubel, D. (1988). Segregation of form, color, movement, and depth: Anatomy, physiology, and perception. *Science, 240,* 740–749.
Lyon, D. C., Nassi, J. J., & Callaway, E. M. (2010). A disynaptic relay from superior colliculus to dorsal stream visual cortex in macaque monkey. *Neuron, 65,* 270–279.
Mahon, B. Z., Kumar, N., & Almeida, J. (2013). Spatial frequency tuning reveals interactions between the dorsal and ventral visual systems. *Journal of Cognitive Neuroscience, 25,* 862–871.
Mahon, B. Z., Milleville, S. C., Negri, G. A. L., Rumiati, R. I., Caramazza, A., & Martin, A. (2007). Action-related properties shape object representations in the ventral stream. *Neuron, 55,* 507–520.
Merigan, W. H., & Maunsell, J. H. R. (1993). How parallel are the primate visual pathways? *Annual Review of Neuroscience, 16,* 369–402.
Orban, G. A., Fize, D., Peuskens, H., Denys, K., Nelissen, K., Sunaert, S., et al. (2003). Similarities and differences in motion processing between the human and macaque brain: Evidence from fMRI. *Neuropsychologia, 41,* 1757–1768.
Osiurak, F., Jarry, C., & Le Gall, D. (2010). Grasping the affordances, understanding the reasoning: Toward a dialectical theory of human tool use. *Psychological Review, 117,* 517–540.
Peeters, R. R., Rizzolatti, G., & Orban, G. A. (2013). Functional properties of the left parietal tool use region. *Neuroimage, 78,* 83–93.
Rizzolatti, G., & Matelli, M. (2003). Two different streams form the dorsal visual system: Anatomy and functions. *Experimental Brain Research, 153,* 146–157.
Sakuraba, S., Sakai, S., Yamanaka, M., Yokosawa, K., & Hirayama, K. (2012). Does the human dorsal stream really process a category for tools? *Journal of Neuroscience, 32,* 3949–3953.
Scheperjans, F., Eickhoff, S. B., Hömke, L., Mohlberg, H., Hermann, K., Amunts, K., et al. (2008). Probabilistic maps, morphometry, and variability of cytoarchitectonic areas in the human superior parietal cortex. *Cerebral Cortex, 18,* 2141–2157.
Scheperjans, F., Hermann, K., Eickhoff, S. B., Amunts, K., Schleicher, A., & Zilles, K. (2008). Observer-independent cytoarchitectonic mapping of the human superior parietal cortex. *Cerebral Cortex, 18,* 846–867.
Schwarzbach, J. (2011). A simple framework (ASF) for behavioral and neuroimaging experiments based on the psychophysics toolbox for MATLAB. *Behavior Research Methods, 43,* 1194–1201.
Talairach, P., & Tournoux, J. (1988). *A stereotactic coplanar atlas of the human brain*. Stuttgart, Germany: Thieme.
Valyear, K. F., & Culham, J. C. (2010). Observing learned object-specific functional grasps preferentially activates the ventral stream. *Journal of Cognitive Neuroscience, 22,* 970–984.
Vingerhoets, G., Acke, F., Vandemaele, P., & Achten, E. (2009). Tool responsive regions in the posterior parietal cortex: Effect of differences in motor goal and target object during imagined transitive movements. *Neuroimage, 47,* 1832–1843.
Xu, X., Ichida, J. M., Allison, J. D., Boyd, J. D., Bonds, A. B., & Casagrande, V. A. (2001). A comparison of koniocellular, magnocellular and parvocellular receptive field properties in the lateral geniculate nucleus of the owl monkey (Aotus trivirgatus). *Journal of Physiology, 531,* 203–218.